probes with the colour developed using NBT/BCIP or Fast Red respectively.

hh up- and downregulation

Constructs to produce mRNAs were made by inserting the full-length surface fish *shh* cDNA into the pSP64T plasmid. In some experiments we injected zebrafish *shh* and *twhh* mRNAs (1:1) made from pT7TS plasmids. The blastomeres of embryos at the 1–4-cell stage were injected with 0.4 ng nl^{-1} (2 nl total volume) *hh* mRNA or control green fluorescent protein mRNA. Embryos were treated with 20–100 μM cyclopamine (5 mM stock solution in 95% ethanol; Toronto Research Chemicals) from 30% epiboly to hatching.

Received 20 May; accepted 19 July 2004; doi:10.1038/nature02864.

1. Ingham, P. W. & McMahon, A. P. Hedgehog signaling in animal development: paradigms and principles. *Genes Dev.* **15,** 3059–3087 (2001).
2. Jeffery, W. R. Cavefish as a model system in evolutionary developmental biology. *Dev. Biol.* **231,** 1–12 (2001).
3. Jeffery, W. R. & Martasian, D. P. Evolution of eye regression in the cavefish *Astyanax*: Apoptosis and the *Pax6* gene. *Am. Zool.* **38,** 685–696 (1998).
4. Yamamoto, Y. & Jeffery, W. R. Central role for the lens in cavefish eye degeneration. *Science* **289,** 631–633 (2000).
5. Jeffery, W. R., Strickler, A. G. & Yamamoto, Y. To see or not to see: Evolution of eye degeneration in the Mexican blind cavefish. *Integr. Comp. Biol.* **43,** 531–541 (2003).
6. Culver, D. C. *Cave Life. Evolution and Ecology* (Harvard Univ. Press, Cambridge, 1982).
7. Mitchell, R. W., Russell, W. H. & Elliot, W. R. Mexican eyeless characin fishes, genus *Astyanax*: Environment, distribution, and evolution. *Spec. Publ. Mus. Texas Tech. Univ.* **12,** 1–89 (1977).

A relative signalling model for the formation of a topographic neural map

Michaël Reber, Patrick Burrola & Greg Lemke

Molecular Neurobiology Laboratory, The Salk Institute, La Jolla, California 92037, USA

The highly ordered wiring of retinal ganglion cell (RGC) neurons in the eye to their synaptic targets in the superior colliculus of the midbrain has long served as the dominant experimental system for the analysis of topographic neural maps[1–3]. Here we describe a quantitative model for the development of one arm of this map—the wiring of the nasal–temporal axis of the retina to the caudal–rostral axis of the superior colliculus. The model is based on

RGC–RGC competition that is governed by comparisons of EphA receptor signalling intensity, which are made using ratios of, rather than absolute differences in, EphA signalling between RGCs[4]. Molecular genetic experiments, exploiting a combinatorial series of EphA receptor knock-in and knockout mice, confirm the salient predictions of the model, and show that it both describes and predicts topographic mapping.

During development, nervous systems are organized into precise representations of the external world[1]. These frequently take the form of a topographic map—an ordering of axonal connections in which the positional coordinates of a set of input neurons are mapped to the corresponding coordinates of their targets. The model for such maps is the projection that connects the RGCs of the eye to their targets in the superior colliculus (SC; referred to as the tectum in non-mammalian vertebrates)[1–3,5]. In this projection, the nasal–temporal (NT) and dorsal–ventral axes of the retina are mapped to the caudal–rostral and lateral–medial axes, respectively, of the SC (Fig. 1a).

The chemoaffinity hypothesis posits that axonal connections within a topographic map may be specified by interacting molecular tags that are distributed in complementary gradients on both projecting axons and their targets[2]. In the retinocollicular map, members of the EphA family of receptor tyrosine kinases, together with their ephrin-A ligands, are thought to function as these graded tags[5–7]. EphA5 and EphA6 are expressed in a low-nasal-to-high-temporal gradient in the mouse retina[4,8], and ephrin-A2 and ephrin-A5 are expressed in a low-rostral-to-high-caudal gradient in the SC[8,9] (Fig. 1a). EphA4 is also expressed by mouse RGCs but is ungraded[4,10–12]. Thus, retinal neurons with the most EphA receptors connect to collicular targets that carry the fewest ephrin-As, and vice versa (Fig. 1a). This is consistent with the demonstration that the ephrin-As are potent chemorepellents for RGC axons, most notably for those that originate in the temporal retina[10,13,14].

We have previously described a set of knock-in mice that permit a quantitative assessment of the role of EphA receptors in retinocollicular mapping[4]. In these mice, the *Islet2* (*Isl2*) gene, which is expressed at a constant level in a subset of RGCs randomly scattered across the retina, was used to drive ectopic expression of the EphA3 receptor[4]. EphA3 is not normally expressed in mouse RGCs[4,8] but binds ephrin-A2 and ephrin-A5 with high affinity[6,12]. The retinocollicular maps that develop in the *Isl2-EphA3* mice suggest that RGCs compete for target sites in the SC through relative, and not absolute, difference comparisons in EphA receptor signalling intensity[4]. If this is indeed so, then the apparent linearity of the mouse retinocollicular map[4] requires that C_v, the concentration per RGC of the two receptors that are graded (EphA5+EphA6), must vary, as a function of position along the retinal axis, in proportion to itself (see Box 1, equation (1)); that is, that the retinal gradient for these receptors must be an exponential[15] (equation (2)). Because C, the summed concentration of all EphA receptors per RGC (ΣEphA), is equal to $C_v + C_4$ (where C_4 is the constant concentration of EphA4), the full EphA gradient should be described by an exponential plus a constant (equation (3)).

To determine whether this is the case, we quantified *EphA4*, *EphA5* and *EphA6* messenger RNA levels in RGCs. (These seem to be the only relevant EphAs in the mouse[4,16].) We performed this quantification across the NT axis of the retina at postnatal day 1 (P1), a time at which RGC competition in the SC is underway[17] (see Methods). We measured mRNAs because the analysis below requires firm numbers for the expression level per RGC of each of the receptor gene products as a function of axial position, and these cannot be obtained for the individual EphA proteins. A typical *in situ* hybridization signal for *EphA6* mRNA is illustrated in Fig. 1b, and *EphA6* mRNA quantification across the NT (x) axis is illustrated in Fig. 1c.

We similarly measured the *EphA4* and *EphA5* mRNAs (Fig. 1d). Like the *EphA6* gradient, that for *EphA5* is nonlinear. When the *EphA5* and *EphA6* points at each axial position are summed, the composite C_v curve that is generated is well fitted by equation (2) (see Box 1), in which C_{v0}, the composite value of *EphA5* + *EphA6* at the nasal pole of the retina ($x = 0$), is 0.26, and $k = 0.023$. (Curve fits were performed with Kaleidagraph, from Synergy Software.) In keeping with previous qualitative assessments[4,10,18,19], we found that RGC expression of *EphA4* mRNA is approximately constant across the NT axis (Fig. 1d). Adding the values at each point of the individual *EphA4*, *EphA5* and *EphA6* curves yields ΣEphA, the aggregate EphA receptor mRNA level per RGC (Fig. 1d, e). The ΣEphA points are well fitted by equation (4) (see Box 1), in which 0.26 is C_{v0}, 0.023 is k, and 1.05 is C_4 of equation (3) (Fig. 1e). The computer-selected C_4 constant is in close agreement with the mean measured value of *EphA4* mRNA (1.08 ± 0.07; Fig. 1d), and the selected C_{v0} constant is in similarly close agreement with the measured nasalmost *EphA5*+*EphA6* mRNA value of 0.30 (Fig. 1d). Thus, the ΣEphA receptor gradient of the mouse retina is indeed modelled by an exponential plus a constant. (See Supplementary Fig. 1 for additional data and discussion.) Note that this gradient is shallow: the difference in ΣEphA between the temporal and nasal poles of the retina is only about 2.75-fold (Fig. 1e).

We also quantified *EphA3* expression in the *EphA3*$^+$ RGCs of P1 *Isl2-EphA3* heterozygous and homozygous knock-ins. We found that the *EphA3* mRNA expressed through the *Isl2* knock-in is approximately constant, and that the heterozygote signal is about 50% of the homozygote signal (Fig. 2a). When the measured *EphA3* 'spikes', corresponding to the subset of RGCs that are *Isl2*$^+$ (ref. 4), are added to the wild-type ΣEphA curve, the quasi-oscillatory EphA gradients of the *Isl2-EphA3* heterozygotes (Fig. 2b) and homozygotes (Fig. 2c) are obtained.

The retinocollicular maps of these mice have been determined previously[4], by using focal retinal injections of the fluorescent axonal tracer 1,1′-dioctadecyl-3,3,3′,3′-tetramethylindocarbocyanine perchlorate (DiI) (Fig. 2d). These label a small cluster of RGCs, which in the *Isl2-EphA3* mice will contain both *EphA3*$^+$ and *EphA3*$^-$ neurons, together with their projecting axons and

Box 1
Relative signalling equations

+/+	$\frac{dC_v}{dx} = kC_v$	(1)
+/+	$C_v(x) = C_{v0}e^{kx}$	(2)
+/+	$C(x) = C_{v0}e^{kx} + C_4$	(3)
+/+	$C(x) = 0.26e^{0.023x} + 1.05$	(4)
ki/+	$C(x) = 0.26e^{0.023x} + 1.98$	(5)
ki/ki	$C(x) = 0.26e^{0.023x} + 2.91$	(6)
ki/+	$R_{lrs}(x) = \frac{0.26e^{0.023x} + 1.98}{0.26e^{0.023x} + 1.05}$	(7)
ki/ki	$R_{lrs}(x) = \frac{0.26e^{0.023x} + 2.91}{0.26e^{0.023x} + 1.05}$	(8)
ki/+A4$^{+/-}$	$C(x) = 0.26e^{0.023x} + 1.44 \quad A3^+$	(9)
ki/+A4$^{+/-}$	$C(x) = 0.26e^{0.023x} + 0.51 \quad A3^-$	(10)
ki/+A4$^{+/-}$	$R_{lrs}(x) = \frac{0.26e^{0.023x} + 1.44}{0.26e^{0.023x} + 0.51}$	(11)
+/+	$R_{grs}(x) = \frac{3.7}{0.26e^{0.023x} + 1.05}$	(12)

C = concentration of ΣEphA (EphA4 + 5 + 6) per RGC; k = constant of proportionality; C_v = concentration of EphA5 + 6 per RGC; $C_{v0} = C_v$ at $x = 0$ (nasal pole of retina) (temporal pole $x = 100$); C_4 = concentration of EphA4 per RGC (constant); R_{lrs} = local relative signalling ratio; R_{grs} = general relative signalling ratio; ki = knock-in.

termination zones (TZs) in the SC[4] (Fig. 2d). The map of *Isl2-EphA3* heterozygotes is duplicated for the nasalmost 76% of the NT axis, but collapses to a single coherent map for the remaining 24% of the retina[4]. That is, adjacent *EphA3*$^+$ and *EphA3*$^-$ RGCs project to separate caudal–rostral collicular positions, with the TZs of *EphA3*$^-$ cells located more caudally, for all injections performed over the first 76% of the NT axis (Fig. 2d). In more temporal locations (77–100% of the axis), adjacent *EphA3*$^+$ and *EphA3*$^-$ RGCs project to a single TZ[4]. Mapping 'collapse' is proposed to occur at 76% of the retinal axis because at this point the ΣEphA expression ratio between adjacent *EphA3*$^+$ and *EphA3*$^-$ RGCs becomes too small for the mapping system to discriminate[4]; in other words, this ratio, which we refer to as the local relative signalling ratio (R_{lrs}), falls below a discrimination limit at this point. (Note that the absolute difference between adjacent *EphA3*$^+$ and *EphA3*$^-$ RGCs does not vary across the NT axis of the knock-ins (Fig. 2a–c).) The quantification of receptor mRNAs allowed us to determine the value of this discrimination limit. The single on/off ΣEphA gradient in the heterozygous knock-ins (Fig. 2b, inset) can be modelled by two smooth-component exponentials—one for the wild-type *EphA3*$^-$ RGCs (equation (4)), and a second for the knock-in *EphA3*$^+$ RGCs. The equation for the *EphA3*$^+$ curve is equation (5) (see Box 1), which has the constant heterozygote level of *EphA3* mRNA (0.93 ± 0.06) added to the C_4 constant of equation (4) (Fig. 2b). Similarly, the exponential that models the *EphA3*$^+$ RGCs in the homozygous knock-ins is equation (6) (see Box 1), where the last constant reflects a further dose of *EphA3* (Fig. 2c).

Dividing equation (5) by equation (4) yields equation (7), the local relative signalling (RS) ratio function for the heterozygous knock-ins. This function, plotted in Fig. 2e, describes how the ΣEphA expression ratio for adjacent (formally, superimposed) *EphA3*$^+$ and *EphA3*$^-$ RGCs varies with position along the NT axis. A collapse point at 76% of the NT axis defines a discrimination limit ratio of 1.36 on this curve (Fig. 2e). If this value is fixed for mice of any genotype, it should not be reached in the *Isl2-EphA3* homozygotes, because these mice display a duplicated retinocollicular map across their entire NT axis[4]. The function that describes R_{lrs} between adjacent *EphA3*$^+$ and *EphA3*$^-$ RGCs in the homozygous knock-ins is equation (8), which is equation (6) divided by

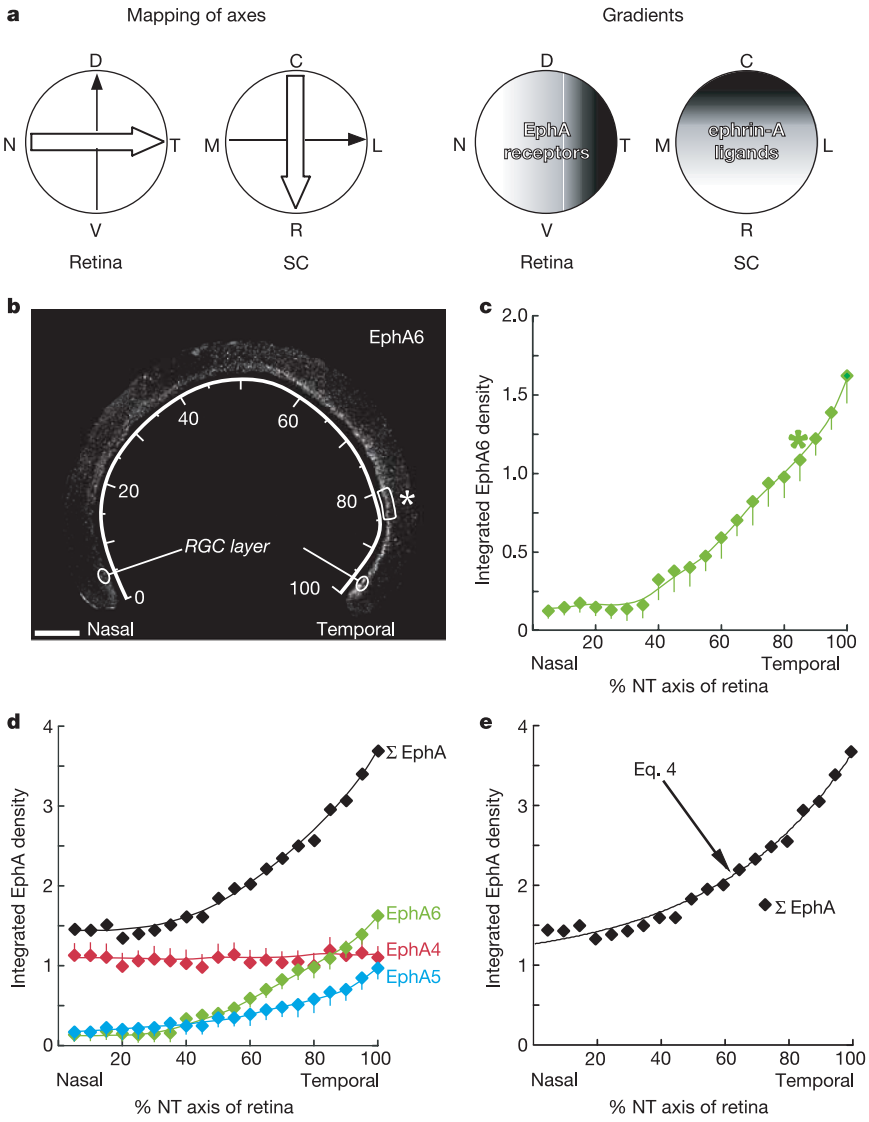

Figure 1 *EphA* mRNAs in the retina. **a**, Mapping of the dorsal–ventral (DV) and nasal–temporal (NT) retinal axes onto the lateral–medial (LM) and caudal–rostral (CR) axes of the SC (left); and EphA receptor and ephrin-A ligand gradients (right). **b**, Section of P1 mouse retina hybridized with an *EphA6* probe. Quantification was performed for 20 segments of the RGC layer (see Methods), one of which is outlined (asterisk). Scale bar, 200 μm. **c**, *EphA6* gradient (integrated signal density for *EphA6*$^+$ RGCs per segment) averaged over seven sections comparable to that in **b**. Asterisk corresponds to the segment in **b**. **d**, *EphA4* ($n = 8$), *EphA5* ($n = 7$) and *EphA6* ($n = 7$) mRNAs, and their summed values (ΣEphA). Error bars in **c** and **d** show one standard deviation from the mean. **e**, The ΣEphA gradient is well fitted by equation (4).

equation (4) (see Box 1). The plot of equation (8) does indeed fail to reach the discrimination limit (Fig. 2f), and thus predicts the fully duplicated map.

We next used mouse knockouts of the *EphA4* gene[20] to generate compound mutants that are trans-heterozygous for both *Isl2-EphA3* and loss of *EphA4*. Removing half of the *EphA4* component from both the numerator and denominator of the local RS ratio in the heterozygous knock-ins predictably increases the value of this ratio across the NT axis (Fig. 3). The ΣEphA gradient of *Isl2-EphA3*$^{ki/+}$*EphA4*$^{+/-}$ mice is illustrated in Fig. 3a. The continous functions that model the *EphA3*$^{+}$ and *EphA3*$^{-}$ components of this gradient are equations (9) and (10) (see Box 1). Dividing equation (9) by equation (10) yields equation (11), the local RS ratio function for these mice. Given a discrimination limit ratio of 1.36, this function predicts that the *Isl2-EphA3*$^{ki/+}$*EphA4*$^{+/-}$ map should be largely duplicated but should still collapse, that the collapse point should be shifted temporally relative to that of *Isl2-EphA3* heterozygotes that are wild type for *EphA4*, and that it should occur at about 88% of the retinal NT axis (Fig. 3b). We generated these *Isl2-EphA3*$^{ki/+}$*EphA4*$^{+/-}$ mice and measured their retinocollicular map (Fig. 3c–e). This map is indeed duplicated throughout most of the retinal axis, but still collapses (Fig. 3e). The collapse point is shifted

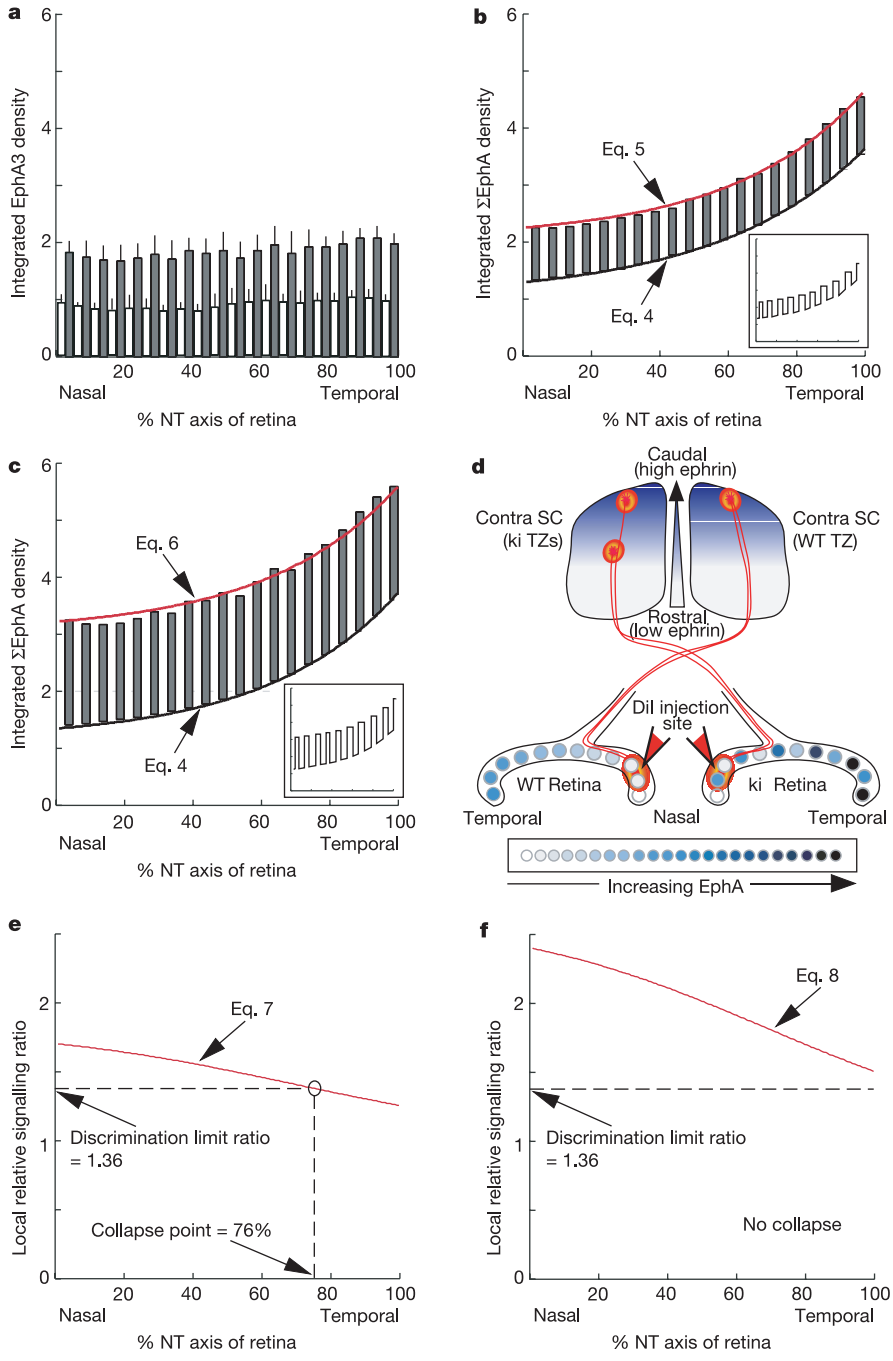

Figure 2 *EphA* expression in the knock-ins. **a**, Discontinuous RGC expression of *EphA3* mRNA in homozygous (ki/ki, grey bars) and heterozygous (ki/+, white bars) knock-ins. Error bars show one standard deviation from the mean ($n = 7$ and $n = 4$ measurements per point for ki/ki and ki/+, respectively). **b**, ΣEphA gradient in *Isl2-EphA3* heterozygotes (ki/+). The ki/+*EphA3* 'spikes' in **a** are superimposed on the curve of equation (4). The red curve (equation (5)) connects the tops of the spikes. The ΣEphA gradient shape is approximated by the inset. **c**, ΣEphA gradient in *Isl2-EphA3* homozygotes (ki/ki). **d**, Results of DiI injection into the nasal retina of wild-type (WT, left) versus knock-in (ki, right) mice. Adjacent WT RGCs with equivalent EphA project to one TZ in the caudal SC, whereas adjacent ki RGCs with different levels of EphA project to two TZs, the more rostral of which corresponds to *EphA3*$^{+}$ RGCs[4]. **e**, **f**, Local RS ratio function in *Isl2-EphA3* heterozygotes (ki/+, **e**) and in homozygotes (ki/ki, **f**).

temporally relative to that observed in heterozygous knock-ins that are wild type for *EphA4*, and now occurs at about 88% of the retinal axis (Fig. 3e).

Note that whereas the separation between $EphA3^{+}$ and $EphA3^{-}$ TZs in the nasal retinae of $Isl2\text{-}EphA3^{ki/+}EphA4^{+/+}$ mice is only on the order of 20% of the caudal–rostral axis of the SC, TZ separation in the $Isl2\text{-}EphA3^{ki/+}EphA4^{+/-}$ mice is much larger (Fig. 3e). This results in the lower map, which corresponds to the TZs of $EphA3^{+}$ RGCs, being compressed into the rostral SC (see Supplementary Fig. 2 and accompanying discussion). This phenomenon is also predicted by relative signalling. At the nasal pole of the retinae of these mice, the ΣEphA ratio between adjacent $EphA3^{+}$ and $EphA3^{-}$ RGCs is 2.2 (Fig. 3b), which is 69% of the operating range of the wild-type retina (1.0–2.75; Fig. 1d). In close correspondence, the separation of the nasalmost pair of duplicated TZs in Fig. 3e is 75% of the collicular axis. The large increase in TZ separation seen in the $Isl2\text{-}EphA3^{ki/+}EphA4^{+/-}$ mice also has important implications for proposed roles for ephrin-A ligands that are expressed in the retina[21] (see Supplementary Information for discussion).

The R_{lrs} functions for each of the three remaining compound genotypes (Fig. 4a, c) make multiple additional predictions, all of which are fulfilled. The R_{lrs} function for $Isl2\text{-}EphA3^{ki/+}EphA4^{-/-}$ mice, for example, predicts a retinocollicular map that is duplicated across nearly the entirety of the retinal NT axis but collapses at the temporal pole (Fig. 4a). This prediction is fulfilled (Fig. 4d). Similarly, the maximal operating range ratio for wild-type mice is exceeded in the nasalmost 30% of the retina in these mice (Fig. 4a), which predicts TZ separations that approach the full extent of the caudal–rostral collicular axis. This is also true (Fig. 4d). The R_{lrs} functions of all three genotypes that are homozygous for *Isl2-EphA3* fail to reach the discrimination limit ratio, irrespective of their *EphA4* genotype (Figs 2e and 4b, c, respectively), and all are therefore predicted to exhibit fully duplicated, non-collapsing maps. Each of these predictions is also fulfilled (Fig. 4e, f; and Fig. 5c in ref. 4).

In the knock-ins, the local RS ratio, which defines a fold difference in ΣEphA between adjacent $EphA3^{+}$ and $EphA3^{-}$ RGCs, accurately predicts the incidence and nasal–temporal position of mapping collapse, as well as the extent of map duplication. However, the local RS ratio in wild-type mice is only trivially different from 1.0, because adjacent RGCs along the wild-type axis have essentially the same level of ΣEphA. So how is it possible for local RS comparisons to be made in the context of the ensemble-wide competition that leads to formation of the wild-type retino-

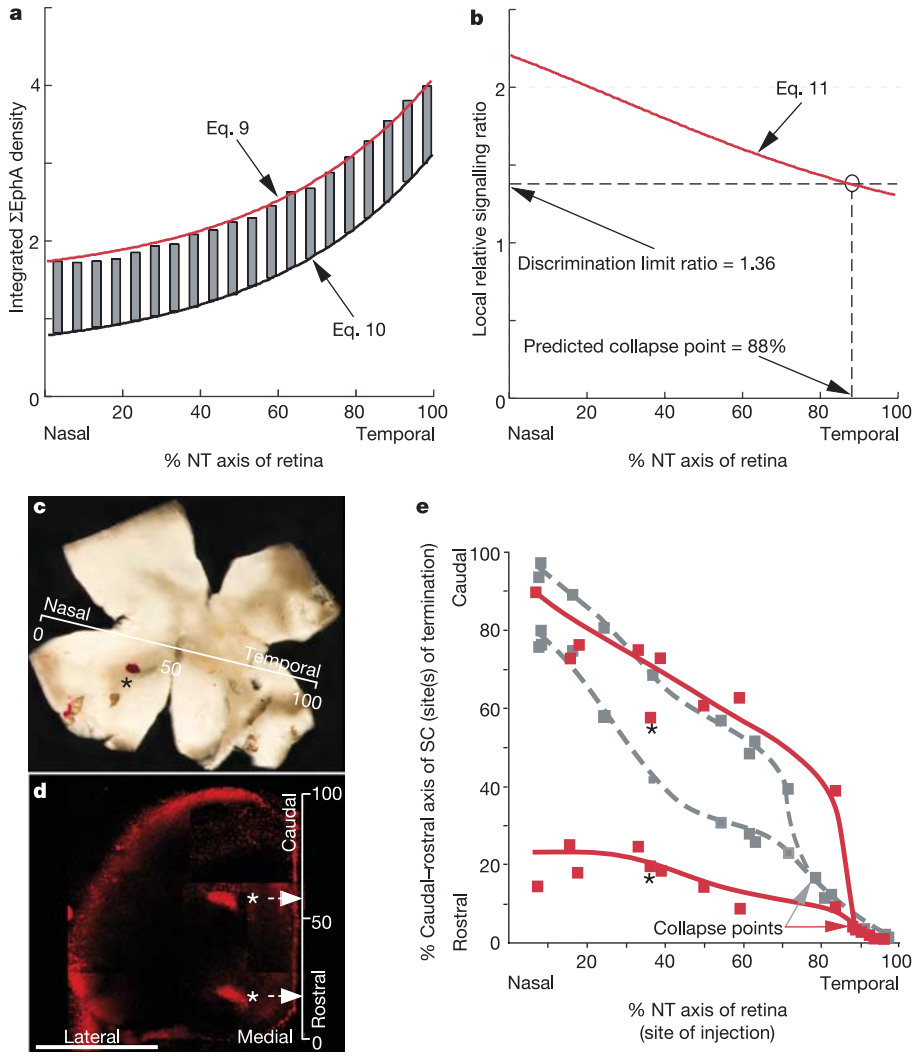

Figure 3 Map perturbation in $Isl2\text{-}EphA3^{ki/+}EphA4^{+/-}$ mice. **a**, ΣEphA gradient in $Isl2\text{-}EphA3^{ki/+}EphA4^{+/-}$ mice. **b**, ΣEphA ratio between adjacent $EphA3^{+}$ and $EphA3^{-}$ RGCs, as a function of retinal position, in these compound heterozygotes. **c**, A P8 retina (flatmount) from these mice, with DiI injected into the ventral nasal quadrant, at 37% of the NT axis (asterisk). **d**, Two TZs (asterisks), at 20% and 58% of the caudal–rostral axis (arrows), labelled in the SC contralateral to the retina in **c**. **e**, Retinocollicular map of $Isl2\text{-}EphA3^{ki/+}EphA4^{+/-}$ mice (red points and curves), determined as in **c** and **d**. Asterisked points correspond to the TZs in **d**. Grey points and curves are from $Isl2\text{-}EphA3^{ki/+}EphA4^{+/+}$ mice[4]. Scale bar, 1 mm.

collicular map? Map formation in most vertebrates takes place during a week-long period of competition between RGC axons for innervation targets in the SC[17,22,23]. If ratiometric comparisons of ΣEphA are used to set the rules by which RGCs compete for a limiting feature of the SC during this time, the dominant cell in the ensemble will be the neuron with the highest levels of ΣEphA signalling and the greatest sensitivity to the collicular ephrin-As; that is, the RGC located at the temporal pole of the retina. (Temporal RGCs are indeed most sensitive to chemorepulsion by ephrin-As[13,19,22,24].) In this milieu, all RGCs might compare themselves with all other RGCs by calculating a general signalling ratio relative to this same temporal reference. (A compelling case for a dominant polar reference cell in 'competition by exclusion' models of retinotectal mapping was—on purely theoretical grounds—made nearly 30 years ago[25].) The highest temporal/nasal ΣEphA ratio (3.7:1.35, or 2.75; Fig. 1e) will characterize RGCs at the nasal pole. Increasingly more temporal RGCs will have increasingly lower ratios, reaching 1.0 at the temporal pole. Most importantly, our model requires that this general relative signalling ratio function provide the algorithm for retinocollicular mapping in wild-type mice. It is expressed by equation (12) (see Box 1), in which the ΣEphA value at the temporal pole of the mouse retina (3.7; Fig. 1e) is divided by the term on the right-hand side of equation (4), which specifies the ΣEphA gradient across the NT axis.

The curve described by equation (12) is plotted in Fig. 5. Although in reality sigmoidal, it is remarkably close to the linear configuration of the wild-type mouse map. When the data points that were used previously to plot this map[4] are superimposed on the curve, there is a nearly perfect correspondence (Fig. 5). Thus, the wild-type retinocollicular map in the mouse is accurately derived from this simple relative signalling rule. It is particularly important to note that the local RS ratio functions of equations (7), (8) and (11) are merely specialized applications of the general RS ratio function of equation (12): the same discrimination limit (1.36) holds for wild-type mice, and the same general ratioing operation applies to the local determination of mapping collapse in the knock-ins, because for two cells RGC_1 and RGC_2, $(3.7/\Sigma EphA_1)/(3.7/\Sigma EphA_2) = \Sigma EphA_2/\Sigma EphA_1$.

Our analyses strongly support the hypothesis that retinocollicular mapping works through relative signalling. By employing the same temporal reference, all RGCs effectively perform a ΣEphA ratio comparison between themselves and all other RGCs. Translation of this ratiometric comparison into competition between RGC axons in the SC might be achieved by one of several mechanisms. One possibility, involving ΣEphA regulation of RGC competiton for brain-derived neurotrophic factor, is described in Supplementary Fig. 3. Note that the reciprocal mapping algorithm of equation (12) accounts for the ability of the wild-type map to discriminate between adjacent RGCs whose local relative signalling ratios are near 1.0: all local comparisons are made in the context of a global comparison with the temporal reference. As we will describe elsewhere, this algorithm also yields the retinocollicular maps of the knock-ins. Although the general RS algorithm has considerable predictive power, our data suggest that ΣEphA gradients on their own do not produce a map that is perfect: in moving nasally from the temporal pole of the retina, the RS discrimination limit of 1.36 is not reached until about 85% of the retinal axis (Fig. 1d). Previously described refinement mechanisms such as coordinated electrical

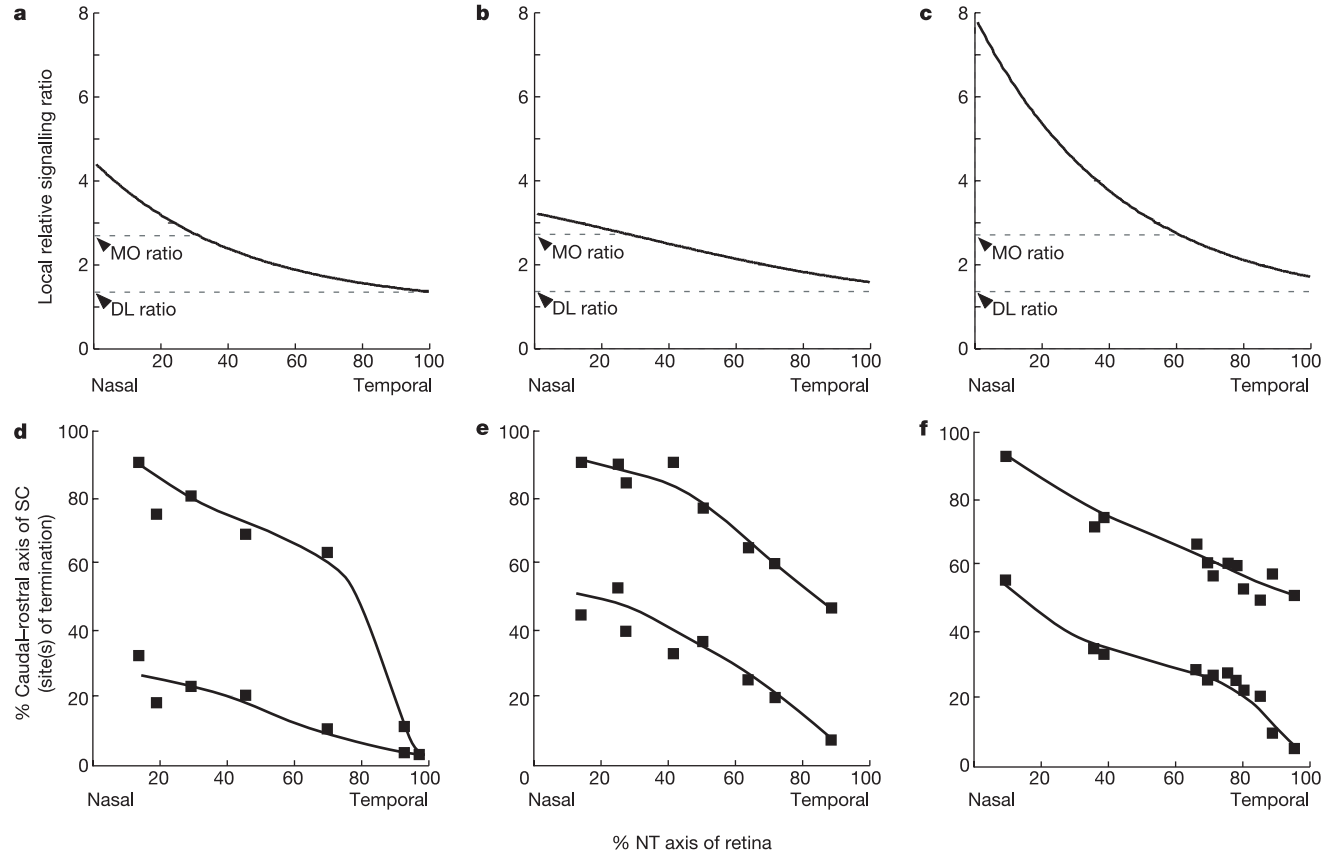

Figure 4 R_{lrs} functions and measured retinocollicular maps in all possible *Isl2-EphA3/EphA4* compound genotypes. **a**–**c**, R_{lrs} functions for *Isl2-EphA3*$^{ki/+}$*EphA4*$^{-/-}$ (**a**) *Isl2-EphA3*$^{ki/ki}$*EphA4*$^{+/-}$ (**b**) and *Isl2-EphA3*$^{ki/ki}$*EphA4*$^{-/-}$ (**c**) mice were calculated by using the measurements and formulations described in the text. For **a**, $R_{lrs}(x) = (0.26e^{0.023x} + 0.90)/0.26e^{0.023x}$; for **b**, $R_{lrs}(x) = (0.26e^{0.023x} + 2.31)/(0.26e^{0.023x} + 0.54)$; for **c**, $R_{lrs}(x) = (0.26e^{0.023x} + 1.80)/0.26e^{0.023x}$. **d**–**f**, Maps for these three genotypes (**d**, **e** and **f**, respectively) were measured by using the methods illustrated in Fig. 3. Discrimination limit (DL; 1.36) and maximal operating (MO; 2.75) ratios are indicated in **a**–**c**.

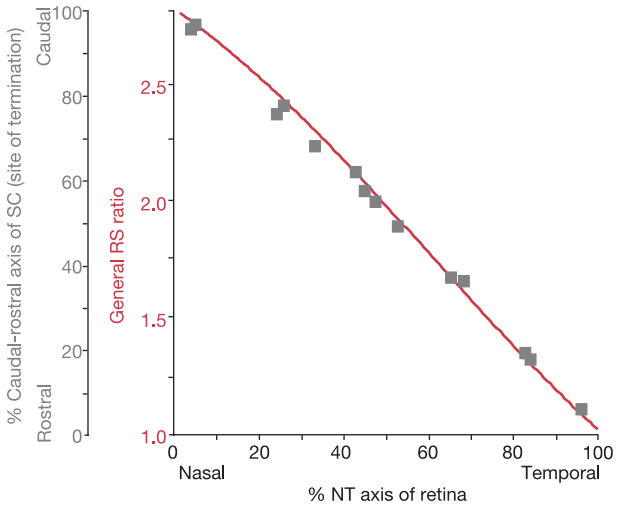

Figure 5 RS derivation of the wild-type map. The red curve (equation (12)) displays the ratio of the ΣEphA value at the temporal pole of the mouse retina (3.7; Fig. 1d) relative to the ΣEphA value across the NT axis. This general RS ratio varies from a nasal maximum of 2.75 to a temporal minimum of 1.0. The offset *y* axis (grey) is the rostral–caudal axis of the SC, and is used to display the previously determined data points of the wild-type retinocollicular map[4].

activity[26], which are unaltered in our mice, must therefore operate to provide ultimate topographic precision.

Gradients of EphA receptors and their ligands are thought to mediate the topographic wiring of multiple other sensory maps in the developing central nervous system[27,28]. More generally, many aspects of neural development, including the survival of neurons based on access to neurotrophins and the stabilization of synapses in the neocortex[29], depend on competition between cells within a developing ensemble. Like retinocollicular innervation, these phenomena are typically dynamic and take place over an extended period. They might also be governed by relative signalling. □

Methods

Quantitative expression analysis

In situ hybridizations with ^{33}P-radiolabelled cRNA probes were performed as described previously[30]. *EphA3*, *EphA4*, *EphA5* and *EphA6* probes were made to the equivalent amino-terminal regions of all four receptors. All probes were between 862 and 927 base pairs in length, contained between 25% and 27% UTP, and were radiolabelled to the same specific radioactivity. Hybridizations were performed at 10^5, 1.5×10^5 and 2×10^5 c.p.m. per slide; these yielded linear increases in signal density across the full NT axis of the retina over the exposure times we employed. Equal probe concentrations were hybridized to adjacent 16-μm horizontal retinal sections, and then emulsion-dipped, developed, and photographed under identical conditions.

Digital images of *in situ* hybridizations were taken at 1,300 × 1,300 resolution. For measurement of signals, the NT axis of the RGC layer of the retina was divided into 20 equal segments; these segments were quantified with the Scion Software (NIH Image version for PC, http://www.scioncorp.com). Positive *in situ* hybridization greyscale signal was counted after removal of a background signal, which was preset after measurement of control sense probe signals by using 'density slicing'. This lower grey detection signal was set at 50 for all quantifications. We performed a more limited set of control measurements with a lower grey threshold of 30, which showed a linear optical response over a 2.5-fold range of detected signal. Using this 30 lower grey threshold, the temporal/nasal fold difference in ΣEphA expression in the retina was, despite the higher absolute signal values, again 2.75-fold. Pixel counts are given in units of 'integrated signal density' (isd, referred to as 'integrated density' on page 37 of the online Scion Image manual). The isd corresponds to the sum of greyscale values for all pixels above the lower grey detection threshold in a given segment (background subtracted). Within a segment, only pixels with signal values above this threshold were scored. Thus, the average area of signal quantification in each segment for hybridizations with *EphA4*, *EphA5* and *EphA6* probes—which detect mRNAs expressed by all RGCs—was approximately twice that of the average area for *EphA3*, which is expressed in about 50% of RGCs in the knock-ins. Neither control sense probes nor regions of the retinal sections that were devoid of cells yielded a positive score using the more than 30 lower grey threshold. The isd values of all plots in this paper are based on the same signal threshold, scale and quantification parameters, and can be compared directly.

Anterograde axon labelling

Focal injections of DiI (Molecular Probes) were made into the left retinae of P7–P8 mice; TZs in the contralateral SC labelled by these injections were analysed 24 h later, as described previously[4,23]. Injected retinae and contralateral SCs were scored, blind to genotype, as whole mounts.

Received 4 June; accepted 9 August 2004; doi:10.1038/nature02957.

1. Kaas, J. H. Topographic maps are fundamental to sensory processing. *Brain Res. Bull.* **44,** 107–112 (1997).
2. Sperry, R. W. Chemoaffinity in the orderly growth of nerve fiber patterns and connections. *Proc. Natl Acad. Sci. USA* **50,** 703–710 (1963).
3. Fraser, S. E. & Hunt, R. K. Retinotectal specificity: models and experiments in search of a mapping function. *Annu. Rev. Neurosci.* **3,** 319–352 (1980).
4. Brown, A. *et al.* Topographic mapping from the retina to the midbrain is controlled by relative but not absolute levels of EphA receptor signaling. *Cell* **102,** 77–88 (2000).
5. O'Leary, D. D. M., Yates, P. A. & McLaughlin, T. Molecular development of sensory maps: representing sights and smells in the brain. *Cell* **96,** 255–269 (1999).
6. Flanagan, J. G. & Vanderhaeghen, P. The ephrins and Eph receptors in neural development. *Annu. Rev. Neurosci.* **21,** 309–345 (1998).
7. McLaughlin, T., Hindges, R. & O'Leary, D. D. Regulation of axial patterning of the retina and its topographic mapping in the brain. *Curr. Opin. Neurobiol.* **13,** 57–69 (2003).
8. Feldheim, D. A. *et al.* Genetic analysis of ephrin-A2 and ephrin-A5 shows their requirement in multiple aspects of retinocollicular map. *Neuron* **25,** 563–574 (2000).
9. Frisén, J. *et al.* Ephrin-A5 (AL-1/RAGS) is essential for proper retinal axon guidance and topographic mapping in the mammalian visual system. *Neuron* **20,** 235–243 (1998).
10. Monschau, B. *et al.* Shared and distinct functions of RAGS and ELF-1 in guiding retinal axons. *EMBO J.* **16,** 1258–1267 (1997).
11. Connor, R. J., Menzel, P. & Pasquale, E. B. Expression and tyrosine phosphorylation of Eph receptors suggest multiple mechanisms in patterning of the visual system. *Dev. Biol.* **193,** 21–35 (1998).
12. Menzel, P., Valencia, F., Godement, P., Dodelet, V. C. & Pasquale, E. B. Ephrin-A6, a new ligand for EphA receptors in the developing visual system. *Dev. Biol.* **230,** 74–88 (2001).
13. Nakamoto, M. *et al.* Topographically specific effects of ELF-1 on retinal axon guidance *in vitro* and retinal axon mapping *in vivo*. *Cell* **86,** 755–766 (1996).
14. Wahl, S., Barth, H., Ciossek, T., Aktories, K. & Mueller, B. K. Ephrin-A5 induces collapse of growth cones by activating Rho and Rho kinase. *J. Cell Biol.* **149,** 263–270 (2000).
15. Goodhill, G. J. Mathematical guidance for axons. *Trends Neurosci.* **21,** 226–231 (1998).
16. Park, S., Frisen, J. & Barbacid, M. Aberrant axonal projections in mice lacking EphA8 (Eek) tyrosine protein kinase receptors. *EMBO J.* **16,** 3106–3114 (1997).
17. Hindges, R., McLaughlin, T., Genoud, N., Henkemeyer, M. & O'Leary, D. D. EphB forward signaling controls directional branch extension and arborization required for dorsal–ventral retinotopic mapping. *Neuron* **35,** 475–487 (2002).
18. Cheng, H. J., Nakamoto, M., Bergemann, A. D. & Flanagan, J. G. Complementary gradients in expression and binding of ELF-1 and Mek4 in development of the topographic retinotectal projection map. *Cell* **82,** 371–381 (1995).
19. Drescher, U. *et al. In vitro* guidance of retinal ganglion cell axons by RAGS, a 25 kDa tectal protein related to ligands for Eph receptor tyrosine kinases. *Cell* **82,** 359–370 (1995).
20. Dottori, M. *et al.* EphA4 (Sek1) receptor tyrosine kinase is required for the development of the corticospinal tract. *Proc. Natl Acad. Sci. USA* **95,** 13248–13253 (1998).
21. Hornberger, M. R. *et al.* Modulation of EphA receptor function by coexpressed ephrinA ligands on retinal ganglion cell axons. *Neuron* **22,** 731–742 (1999).
22. Yates, P. A., Roskies, A. L., McLaughlin, T. & O'Leary, D. D. Topographic-specific axon branching controlled by ephrin-As is the critical event in retinotectal map development. *J. Neurosci.* **21,** 8548–8563 (2001).
23. Simon, D. K. & O'Leary, D. D. M. Development of topographic order in the mammalian retinocollicular projection. *J. Neurosci.* **12,** 1212–1232 (1992).
24. Walter, J., Kern-Veits, B., Huf, J., Stolze, B. & Bonhoeffer, F. Recognition of position-specific properties of tectal cell membranes by retinal axons *in vitro*. *Development* **101,** 685–696 (1987).
25. Prestige, M. C. & Willshaw, D. J. On a role for competition in the formation of patterned neural connections. *Proc. R. Soc. Lond. B* **190,** 77–98 (1975).
26. McLaughlin, T., Torborg, C. L., Feller, M. B. & O'Leary, D. D. Retinotopic map refinement requires spontaneous retinal waves during a brief critical period of development. *Neuron* **40,** 1147–1160 (2003).
27. Feldheim, D. A. *et al.* Topographic guidance labels in a sensory projection to the forebrain. *Neuron* **21,** 1303–1313 (1998).
28. Cutforth, T. *et al.* Axonal ephrin-As and odorant receptors. Coordinate determination of the olfactory sensory map. *Cell* **114,** 311–322 (2003).
29. Cohen-Cory, S. The developing synapse: construction and modulation of synaptic structures and circuits. *Science* **298,** 770–776 (2002).
30. Mui, S. H., Hindges, R., O'Leary, D. D., Lemke, G. & Bertuzzi, S. The homeodomain protein Vax2 patterns the dorsoventral and nasotemporal axes of the eye. *Development* **129,** 797–804 (2002).

Supplementary Information accompanies the paper on **www.nature.com/nature**.

Acknowledgements We thank C. F. Stevens for mathematical insights; M. Dottori and S. Pfaff for the *EphA4* mutants and *Isl2-rlacZ* mice, respectively; D. O'Leary, T. McLaughlin and R. Hindges for discussions and advice on DiI injections; T. Jessell, C. Kintner, M. Meister, S. Pfaff and L. Wolpert for comments on the manuscript; and J. Hash for excellent technical assistance. This work was supported by grants from the NIH (G.L.), the Philippe Foundation (M.R.), and the Bettencourt–Schueller Foundation (M.R.). M.R. was a fellow from Fondation pour la Recherche Medicale.

Competing interests statement The authors declare that they have no competing financial interests.

Correspondence and requests for materials should be addressed to G.L. (lemke@salk.edu).